Latest advancements in imaging techniques in OA

Daichi Hayashi, Frank W. Roemer (iD) **, Thomas Link** (iD) **, Xiaojuan Li, Feliks Kogan, Neil A. Segal, Patrick Omoumi and Ali Guermazi** (iD)

Abstract: The osteoarthritis (OA) research community has been advocating a shift from radiography-based screening criteria and outcome measures in OA clinical trials to a magnetic resonance imaging (MRI)-based definition of eligibility and endpoint. For conventional morphological MRI, various semiquantitative evaluation tools are available. We have lately witnessed a remarkable technological advance in MRI techniques, including compositional/physiologic imaging and automated quantitative analyses of articular and periarticular structures. More recently, additional technologies were introduced, including positron emission tomography (PET)-MRI, weight-bearing computed tomography (CT), photon-counting spectral CT, shear wave elastography, contrast-enhanced ultrasound, multiscale X-ray phase contrast imaging, and spectroscopic photoacoustic imaging of cartilage. On top of these, we now live in an era in which artificial intelligence is increasingly utilized in medicine. Osteoarthritis imaging is no exception. Successful implementation of artificial intelligence (AI) will hopefully improve the workflow of radiologists, as well as the level of precision and reproducibility in the interpretation of images.

Correspondence to:
Ali Guermazi
Department of Radiology, Chobanian & Avedisian School of Medicine, Boston University, Boston, MA 02132, USA

Department of Radiology, VA Boston Healthcare System, U.S. Department of Veterans Affairs, West Roxbury, MA 02132, USA
guermazi@bu.edu

Daichi Hayashi
Department of Radiology, Renaissance School of Medicine at Stony Brook University, Stony Brook, NY, USA

Department of Radiology, Chobanian & Avedisian School of Medicine, Boston University, Boston, MA, USA

Frank W. Roemer
Department of Radiology, Chobanian & Avedisian School of Medicine, Boston University, Boston, MA, USA

Department of Radiology, Universitätsklinikum Erlangen, Friedrich-Alexander-Universität Erlangen-Nürnberg (FAU), Erlangen, Germany

Thomas Link
Department of Radiology, University of California San Francisco, San Franciso, CA, USA

Xiaojuan Li
Department of Radiology, Cleveland Clinic Lerner College of Medicine, Cleveland, OH, USA

Introduction

Imaging of osteoarthritis (OA) has traditionally been dominated by conventional radiography. The OA research community has been advocating the use of a more advanced imaging modality, namely magnetic resonance imaging (MRI), for both epidemiological and clinical research studies of OA. For conventional morphological MRI, various semiquantitative evaluation tools have been developed.[1–3] A recent technological advance in compositional MRI techniques enables the assessment of the physiological status of articular cartilage and other tissues before macroscopically appreciable morphological changes/damage occur.[4] Automated quantitative measurements and segmentation can be performed for not only articular cartilage but also for other articular and periarticular structures. More recently, additional technologies were introduced, including positron emission tomography (PET)-MRI, weight-bearing computed tomography (WBCT),

photon-counting spectral CT, advanced ultrasound techniques such as shear wave elastography and contrast-enhanced ultrasound, multiscale X-ray phase contrast imaging, and spectroscopic photoacoustic imaging of cartilage. Research papers describing the use of artificial intelligence (AI) in the imaging of OA are increasingly available. In this narrative review article, we describe the latest advancements in the multimodality imaging techniques of OA that are primarily used in the research setting, mainly focusing on the literature evidence published over the last 5 years. Older publications are also cited when they are relevant for the discussion of the subject matter.

Recent developments in semiquantitative and quantitative MRI of OA

Semiquantitative MRI evaluation of articular and periarticular structures in OA is commonly

Feliks Kogan
Department of Radiology, Stanford University, Stanford, CA, USA

Neil A. Segal
Department of Rehabilitation Medicine, The University of Kansas, Kansas City, KS, USA

Patrick Omoumi
Department of Radiology, Lausanne University Hospital, University of Lausanne, Lausanne, Switzerland

Table 1. Summary of MOAKS, ACLOAS, and ROAMES.

Semiquantitative scoring systems	Purpose	Features assessed
MRI OsteoArthritis Knee Scoring System (MOAKS)	MRI-based whole-joint evaluation of the knee OA features	Cartilage damage (area and depth), bone marrow lesions (size and % of cystic area), meniscus morphology and extrusion, osteophytes, Hoffa-synovitis, effusion-synovitis
Anterior Cruciate Ligament OsteoArthritis Scoring (ACLOAS)	MRI-based assessment of ACL injury and follow-up of structural sequelae	Cartilage damage, osteochondral injury type and size, traumatic and degenerative bone marrow lesions, meniscal morphology and extrusion, osteophytes, ligaments and ACL graft, Hoffa-synovitis, effusion-synovitis
Rapid OsteoArthritis MRI Eligibility Score (ROAMES)	A simplified MRI instrument for defining structural eligibility of patients for inclusion in disease-modifying OA drug trials using a tri-compartmental approach that enables stratification of knees into different structural phenotypes and includes diagnoses of exclusion	Cartilage damage, bone marrow lesions (size and % of cystic area), meniscus morphology and extrusion, osteophytes, Hoffa-synovitis, effusion-synovitis, phenotypic stratification (inflammatory, mechanical, bone, atrophic, hypertrophic), diagnoses of exclusion

ACL, anterior cruciate ligament; MRI, magnetic resonance imaging; OA, osteoarthritis.

performed. It helps researchers gain a deeper understanding of the pathophysiology and natural history of OA. The most commonly studied joint is the knee, for which several semiquantitative scoring systems are available. The three most recently developed scoring systems that evaluate the whole knee joint are MRI OsteoArthritis Knee Score (MOAKS),[1] Anterior Cruciate Ligament OsteoArthritis Score (ACLOAS),[2] and Rapid OsteoArthritis MRI Eligibility Score (ROAMES).[3] These scoring systems have been used in epidemiological knee OA studies (Table 1). A case-control study based on Osteoarthritis Initiative (OAI) data showed worsening MOAKS scores of effusion-synovitis were highly associated with knee OA progression over a 4-year period, particularly among obese individuals [odds ratio (OR) 34.1; 95% confidence interval (CI) 4.2–274.8, $p = 0.001$].[5] A retrospective cohort study, also using the OAI database, found a positive association between sustained knee synovitis (scored by ACLOAS and MOAKS) and greater progression of cartilage abnormalities related to OA.[6]

Another OAI-based study showed statin therapy in patients for cardiovascular disease-related indications may be protective against OA-related subchondral bone marrow lesions assessed by MOAKS in individuals with generalized OA phenotype.[7] ROAMES proposed the following phenotypes of OA: inflammatory, meniscus/cartilage, subchondral bone, atrophic, and hypertrophic, reflecting predefined stratification based on MOAKS. Using ROAMES on OAI data (2,328 participants without radiographic OA at baseline), Lee *et al.*[8] showed inflammatory, meniscus/cartilage, and subchondral bone phenotypes were associated with time to radiographic OA ($p < 0.05$). Female subjects with hypertrophic phenotype were associated with 2.8 times greater risk of radiographic OA (95% CI 2.25–7.54) compared with male subjects without hypertrophic phenotype. Figure 1 shows illustrative examples of the different ROAMES phenotypes.

Quantitative measurement of articular structures, such as cartilage, menisci, synovium, and
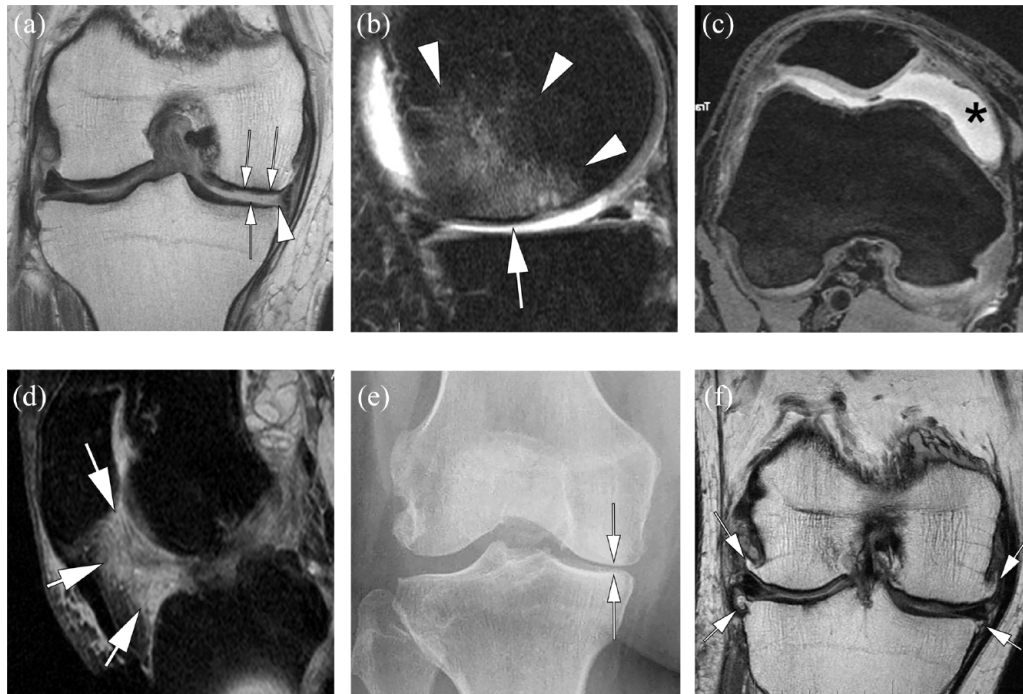
Figure 1. Phenotypic characterization. (a) The cartilage/meniscus phenotype is characterized by severe meniscal damage depicted in this example as partial meniscal maceration of the medial meniscal body (arrowhead) and commonly associated with severe cartilage loss (arrows point to diffuse superficial cartilage damage of the medial tibia and femur). Different definitions of a cartilage-meniscus phenotype have been proposed depending on the amount of cartilage damage and meniscal involvement.[9] (b) Bone phenotype. A large bone marrow lesion (BML) is present in the medial central subregion of the medial femur (grade 3, arrows). The size of the BML defines this knee as a subchondral bone phenotype. (c) The inflammatory phenotype is characterized by severe joint effusion-synovitis (asterisk). (d) So-called Hoffa-synovitis, a nonspecific surrogate of whole knee synovitis, is another manifestation of inflammation and is considered for the classification of an inflammatory structural phenotype. (e) The atrophic phenotype is characterized by severe cartilage loss without relevant osteophyte formation. It can be diagnosed by radiography. Anterior-posterior radiograph shows severe medial joint space narrowing (arrows) defining this knee as Kellgren–Lawrence grade 3. The discrepancy between joint space narrowing (a surrogate for cartilage and meniscal damage, and meniscal extrusion) defines this knee as having an atrophic phenotype. (f) The hypertrophic phenotype is characterized by large osteophytes with only minor cartilage loss. Of the five suggested phenotypes also the hypertrophic phenotype can be diagnosed by X-ray, acknowledging that joint space narrowing is a composite structural manifestation of disease. The coronal intermediate-weighted image shows large osteophytes at the medial and lateral femoral joint margin (arrows) and moderate-sized osteophytes at the medial and lateral tibia (arrowheads).

infrapatellar fat pad (IFP), allows the evaluation of morphologic tissue parameters as continuous variables. A novel application of diffusion tensor imaging (DTI) for imaging of synovitis in knee OA has been reported.[10] The gold standard of synovitis imaging has been the use of dynamic contrast-enhanced (DCE)-MRI parameter K^{trans} which enabled quantification of the intensity of synovial inflammation in knees with OA. However, the need for the use of intravenous injection of gadolinium-based contrast agent has prevented the routine clinical or research use of DCE-MRI for synovitis assessment in knee OA. Sandford *et al.*[10] used two quantitative parameters, that is, mean diffusivity (MD) and fractional anisotropy (FA) and found that MD was significantly positively correlated with K^{trans} ($p < 0.001$), while FA was significantly negatively correlated with K^{trans} ($p < 0.0026$). This study thus indicated DTI-based quantitative measures of the intensity of synovitis may provide additional information in addition to morphologic evaluation of OA severity. A different study also attempted to evaluate synovitis in knee OA without the use of gadolinium contrast.[11] A linear combination of two quantitative double-echo in steady state (qDESS) images was used to create an image which shows contrast between synovium and the synovial fluid.

Synovitis sum scores of the whole knee on qDESS MRI and CE-MRI had a very strong correlation ($p < 0.001$) with high absolute agreement (0.84; 95% CI 0.14–0.95). However, qDESS was shown to systematically underestimate synovitis severity compared with CE-MRI. Moreover, double-inversion recovery (DIR) technique with synthetic MRI using two inversion times (280–330 ms and 2800–2900 ms) was developed and compared with T1-weighted CE-MRI for the assessment of knee synovitis.[12] Synthetic DIR showed a moderate degree of interobserver agreement and good accuracy for detecting synovitis, demonstrating its potential utility in situations when synovitis assessment is required without CE-MRI.

Finally, three recent studies reported quantitative MR evaluation of the IFP in knee OA.[13–15] Zhong *et al.*[13] investigated the characteristics of fat content and component in IFP by means of hydrogen proton MR spectroscopy (1 H-MRS) in knee OA. Alteration of fat fraction in IFP was associated with the radiographic severity of knee OA, MOAKS-based synovitis, and knee pain. Chen *et al.*[14] evaluated fat fraction and T2* relaxation based on DIXON MRI of IFP in older adults with knee OA. Fat fraction and T2* relaxation values decreased as the severity of radiographic OA increased. Li *et al.*[15] performed a prospective nested case-control study including 690 participants with knees at the risk of OA from the Pivotal OA Initiative MRI Analyses incident OA cohort. The study showed MRI-based three-dimensional (3D) texture analysis of IFP was associated with future development of knee OA. Quantitative parameters related to IFP may serve as a new imaging biomarker for knee OA severity assessment based on MRI.

Compositional MR imaging of cartilage

Compositional MR imaging techniques have been developed to analyze cartilage matrix quality before cartilage is lost and to diagnose cartilage damage which is at its early stages and potentially reversible.[16] At this stage, management strategies and lifestyle modifications may be instituted, which may halt disease progression and decrease disease burden.[17] A number of MRI-based technologies have been developed which can be used to characterize different components of the cartilage matrix such as collagen, water content, and proteoglycans; these include T_2, T_2*, and $T_1\rho$ relaxation time measurements as well as delayed gadolinium-enhanced MRI of cartilage (dGEMRIC), sodium imaging, and glycosaminoglycan (GAG)-specific chemical exchange saturation transfer (gagCEST).[18,19] To date, most clinical data are available for T_2 and $T_1\rho$ mapping, which have been shown to provide information on collagen integrity and water and proteoglycan content;[16] these measures have also been shown to predict radiographic OA and disease progression.[20–22] dGEMRIC has been used in multiple clinical studies and has been shown to quantify proteoglycan content, but it requires gadolinium contrast administration.[23,24] Sodium imaging and gagCEST are promising technologies but are primarily dependent on ultra-high field strength and sophisticated software and hardware, which will be challenging to implement in clinical practice.[25,26] Diffusion-weighted imaging (DWI) and DTI as well as ultrashort TE (UTE) imaging can be used to assess water molecules, collagen matrix, and proteoglycans within the cartilage. Increased apparent diffusion coefficient values indicate cartilage degeneration.[27] UTE imaging is useful for the evaluation of calcified cartilage.[27]

The development of cartilage compositional imaging techniques has been hampered by several factors. These include the interpretation of values, intra- and inter-individual variabilities, the influence of vendors and the hardware, and software that makes comparability challenging, as well as the long MRI acquisition times and time-consuming analysis techniques, which have in the past made it challenging to use these techniques outside of research applications.[28] There have been some recent developments, which have improved the feasibility to use these techniques in a clinical environment including the implementation of *fast acquisition techniques*, as described below.[29–33] Different technologies have been used which include parallel imaging, compressed sensing (CS), and deep learning-based reconstruction algorithms. The combination of parallel imaging and CS has been found to be useful in accelerating cartilage $T_1\rho$ acquisition with acceleration factors up to 8–10.[29–31] MR fingerprinting is a new method that allows simultaneous measurement of multiple tissue properties in a single time-efficient acquisition. Previous studies have shown that this technology can analyze multiple cartilage MR parameters such as T_2 and $T_1\rho$ at the knee simultaneously.[32] Very recently, researchers have applied deep learning-based reconstruction techniques to accelerate the
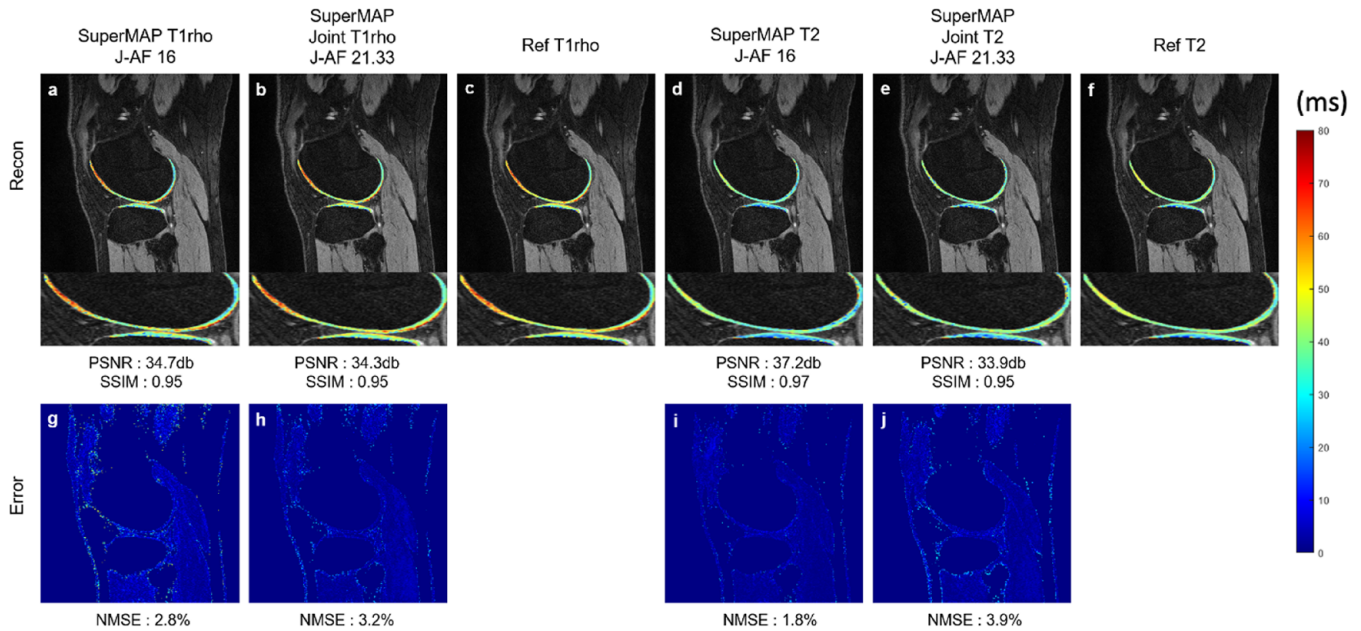
Figure 2. $T_1\rho$ and T_2 maps reconstructed from prospectively under-sampled data using a novel deep learning-based reconstruction framework (termed as 'SuperMAP'). SuperMAP incorporates batchwise training with the entire image as the backward cycle (model-data) for consistency, and directly converts a series of under-sampled (both in k-space and parameter-space) T2- and $T_1\rho$-weighted images into T_2 and $T_1\rho$ maps, bypassing the conventional exponential fitting procedure. SuperMAP exploits both spatial and temporal information and generates $T_1\rho$ (a) and T_2 (d) maps with high acceleration factors (AF = 16). Furthermore, the deep learning model were trained to simultaneously reconstruct $T_1\rho$ (b) and T_2 (e) maps from combined $T_1\rho$ and T_2 acquisition within a single scan with higher acceleration factors (AF = 21.33). T_2 and $T_1\rho$ maps generated from both methods had small errors (g, h) (i, j) and high agreement to reference maps (c, f). Such techniques will allow $T_1\rho$ and T_2 imaging of the whole knee within less than 1 min. Source: Figure from Zhou *et al.*[29] with permission.

acquisition of cartilage T_2 and $T_1\rho$ imaging.[33] High acceleration factors (>16) were achieved for both retrospective and prospective under-sampled data with a high agreement with the reference maps (Figure 2).[33]

In the past, cartilage segmentation required to quantify cartilage composition took 30 min to several hours per knee MRI and was impractical for analysis of larger datasets or clinical practice. Recently, however, cartilage segmentation and analysis have been significantly improved by novel *artificial intelligence-based cartilage segmentation and analysis tools*. In a recent study, Razmjoo *et al.*[22] used a machine learning-based segmentation model for automatic cartilage segmentation of the entire osteoarthritis initiative (OAI) data set and calculated T_2 relaxation time values in 4796 research subjects, which also included longitudinal acquisitions and resulted in T_2 values of 25,729 knee MRI studies in total. These researchers found that T_2 values calculated with the

machine learning model were comparable with those obtained by manual segmentation. They also found that individuals in the highest 25% quartile of tibio-femoral T_2 values had a five times higher risk of radiographic OA incidence after 2 years and confirmed the predictive value of T_2 measurements for future incidence of radiographic OA. Other studies also demonstrated feasibility and good performance of machine-learning based cartilage segmentation in knee MRI data sets.[34–38]

In summary, MRI-based compositional imaging of cartilage can provide pertinent information about cartilage quality and show early evidence of cartilage damage before cartilage tissue is lost. Recent developments accelerating MR image acquisition and automating cartilage tissue segmentation have made it more feasible to use this technology to analyze larger imaging data sets. Additional efforts for standardization of compositional MRI techniques may eventually lead to their clinical application.
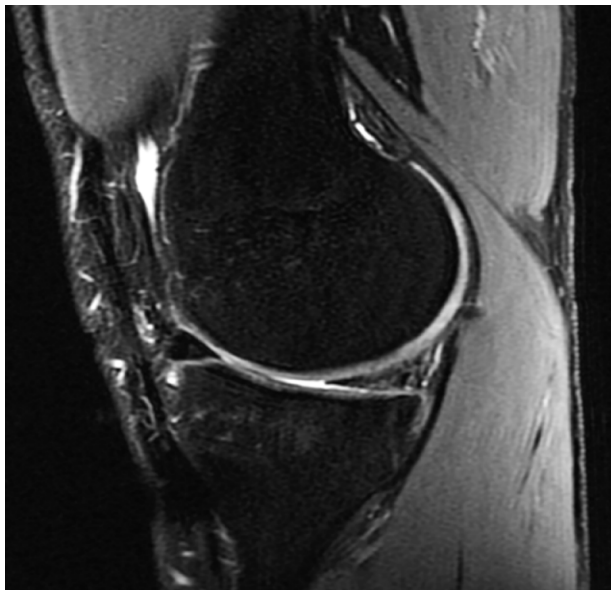
Figure 3. T2-weighted FSE MRI (Left) and [18 F]NaF PET-MRI fusion images of a 23-year-old male subject 2.0 years after ACL tear and reconstructive surgery as well as partial meniscectomy. Increased [18 F]NaF uptake, indicative of bone metabolism, is seen in the ACLR in areas of BML (Purple Arrow) and adjacent meniscal damage (Green Arrow) as well as several regions that appear unremarkable on MRI (Blue arrows). Cartilage morphology and subchondral bone uptake in the contralateral leg appears unremarkable.

PET-MRI in OA imaging

As the assessment of multiple tissue types and functional processes is necessary to evaluate the complex pathogenesis of OA and potential disease-modifying therapies, there has been a new interest in the application of metabolic imaging with PET to OA. PET offers unique abilities to provide quantitative information about molecular and metabolic activities, such as bone remodeling and inflammation, which are thought to be targets of disease-modifying OA therapies. Furthermore, hybrid PET-MRI systems, which have been around now for 10 years, not only offer to add these important functional imaging markers to benchmark MRI morphologic and microstructural soft-tissue markers, but also to study how these different features interact in disease onset and progression.[39,40]

18 F-Sodium Fluoride ([18 F]NaF), which is taken up in areas of newly mineralizing bone and has been shown to correlate with bone histomorphometry, has been the primary PET tracer applied to studying OA due to its unique ability to interrogate bone remodeling. Increased subchondral bone metabolic activity has been shown in the knee regions of OA subjects with osteophytes, BMLs, and adjacent cartilage lesions on MRI.[41–45] Even more striking, significantly increased subchondral bone metabolic activity was seen in regions of normal-appearing bone and adjacent cartilage an OA-group compared with healthy controls.[43] Furthermore, in patients with unilateral anterior cruciate ligament (ACL) tears, significantly increased [18 F]NaF uptake was observed in the subchondral bone of ACL-injured joints, compared with their uninjured contralateral knees.[47] Patients with ACL tears are at a known increased risk for developing OA.[46] These findings support the notion that increased metabolic bone activity detected with [18 F]NaF PET may serve as a marker for abnormal bone remodeling in early OA. Paired with quantitative measures of cartilage microstructure from MRI, [18 F]NaF PET-MRI has been applied to study between-tissue interactions in OA. Increased [18 F]NaF PET uptake has been shown to correlate with increased adjacent cartilage T2 and T1ρ relaxation times in OA at multiple disease stages in the knee and the hip.[42,47–49] In addition, [18 F]NaF PET-MRI imaging, utilizing [18 F]NaF PET as a marker of bone metabolism and dynamic contrast-enhanced (DCE)-MRI as a marker of synovial inflammation, was synergistically utilized to provide direct *in vivo* evidence of associations between synovitis and adjacent metabolic bone activity and osteophyte formations.[50]

[18 F]NaF PET has also been proposed as a marker of whole-joint function (Figure 3). Acute loading, after an exercise protocol, has been shown to alter the bone physiology affecting [18 F] NaF kinetics in both healthy[51] and OA subjects.[52] In addition, correlations of [18 F]NaF uptake induced by exercise with finite element models and generalized joint forces in performed exercises suggest a localized response that may be load-dependent.[51–53] Furthermore, preliminary longitudinal data suggest [18 F]NaF uptake after exercise may be sensitive to regions where there are functional abnormalities in joint response that are at risk of OA progression.[54]

Finally, PET-MRI has seen early applications in identifying sources of musculoskeletal pain. Pain is not only a key driver of doctor visits in OA but joint pain in young adults, such as patellofemoral pain, is also linked to the development of OA. However, diagnosis of pain sources remains
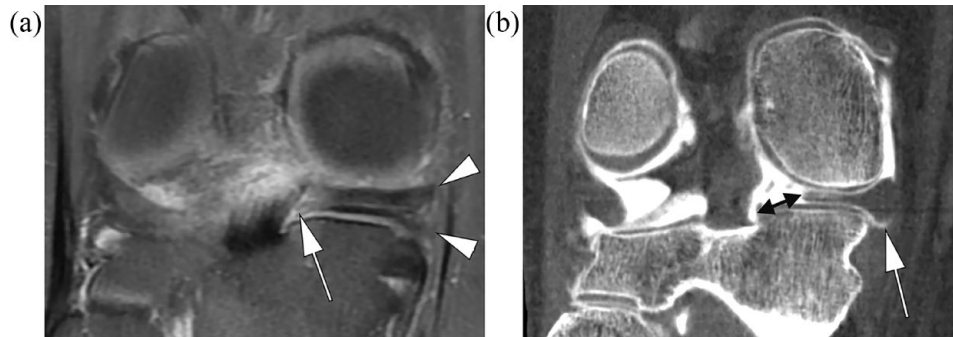
Figure 4. (a) Coronal proton-density-weighted MRI depicting medial meniscal boundary in line with the tibial plateau and no signs of extrusion of the meniscal body (arrows). The root of the posterior horn of the medial meniscus appears thinned but without evidence of a definite tear. (b) Weight-bearing CT arthrography (WBCTa) demonstrates substantial extrusion of the medial meniscus beyond the tibial plateau (arrow). Weight-bearing imaging also reveals a complete tear of the root of the posterior tibial attachment of the medial meniscus with a wide gap (double headed arrow). WBCTa added clinical value by visualizing the cause of the patient's persistent pain and informed the patient's care plan.

challenging due to its subjective nature, localization challenges and the natural variation of morphology and edema in subjects on MRI. PET radiotracers targeting upregulation of receptors and inflammatory cells have been proposed to identify peripheral pain generators. 18-fluorodeoxyglucose ($[^{18}$F]FDG) uptake has been correlated with OA severity as well as applied to early studies of patellofemoral pain sources and total knee arthroplasty.[55,56] Furthermore, a more specific marker of sigma-1 receptor ($[^{18}$F]FTC-146) upregulation has been developed and applied to knee pain in OA.[57] This application may present the most direct clinical translational opportunity for PET-MRI in musculoskeletal disorders.

In summary, multimodality imaging with PET-MRI offers many advantages and new applications for diagnosis, pathogenesis, and treatment monitoring in OA. While technical challenges do exist, the key metric that will determine the utility of these systems will be continued demonstration of unique and clinically valuable applications that can justify the cost and complexity of these systems.

Weight-bearing knee CT in OA imaging

The principal symptom that leads patients to seek clinical care for lower limb OA is pain on weight-bearing. Although standing radiography has been the imaging modality of choice for knee, foot, and ankle OA, 2D radiographs are limited in their abilities to visualize features of OA, making radiographic imaging biomarkers less accurate, sensitive, and responsive than those for 3D imaging

modalities. WBCT has been found to detect signs of OA incidence and progression missed by other imaging modalities.

At the knee, weight-bearing alters the meniscal position and configuration, cartilage compression and apposition, and muscle forces, which alter tibiofemoral joint space width and patellar position. Introduction of low-dose WBCT has offered improved detection of features of knee OA,[58] and enhanced accuracy for detecting hindfoot, midfoot, and ankle OA progression.[59] The absence of bony overlap allows WBCT to avoid problems with beam angle and positioning that have limited radiographs.

For example, Fritz *et al.*[60] reported bone-on-bone apposition in 25% of tibiofemoral compartments using WBCT, in comparison with only 8% and 10%, respectively, on fixed-flexion radiographs (FF-XR) and supine CT. Studies to date, comparing FF-XR and WBCT with MRI have revealed that the sensitivity, accuracy, and predictive value for detecting osteophytes and subchondral cysts is higher on WBCT than on FF-XR;[58] 2D JSW on FF-XR poorly correlates with MRI cartilage damage;[61] 3D joint space width (JSW) on WBCT correlates better than FF-XR with cartilage damage;[62] and responsiveness of change in 3D JSW on WBCT over 24 months is significantly higher than that for radiographic or MRI biomarkers. In addition to 3D JSW on WBCT being more sensitive and responsive to tibiofemoral changes, using articular cartilage morphology on MRI as the referent standard, tibiofemoral 3D

JSW on WBCT correlated more highly than FF-XR minimal JSW;[62] and sensitivity and accuracy for patellofemoral cartilage lesions was significantly higher on WBCT than on FF-XR.[63] Advantages of WBCT are not limited to bony features, in that WBCT visualizes meniscal extrusions not visualized on FF-XR and demonstrates greater severity of extrusion than has been detected on supine MRI.[64] Given that 60% to 80% of knees with greater meniscal extrusion visualized on WBCT than on MRI are Kellgren and Lawrence (KL) grade 0–1, WBCT could be instrumental in identifying early OA. Contrast enhancement with WBCT arthrography has allowed detection of meniscal tears not visualized on MRI, further strengthening the ability to detect early OA (Figure 4).

While the knee is the most common weight-bearing joint affected by OA, foot and ankle OA detection has also benefited by the introduction of more accurate WBCT assessments of structural risk factors for OA development. For example, weight-bearing cross-sectional imaging has clarified clinically meaningful subtalar joint anatomy not visualized on conventional radiography.[59] Furthermore, WBCT has been more accurate than radiographs for assessing hind- and midfoot measurements. Since hindfoot alignment also affects tibiotalar OA, more accurate measurements of ankle OA could guide surgical indications.[65]

These advantages have contributed to WBCT enhancing earlier detection, longitudinal monitoring, and management of lower limb OA. WBCT imaging biomarkers also may improve patient stratification by characterizing OA features not visualized on other modalities. Given the aging of the population, early detection of OA is essential to reduce disablement. Thus, WBCT holds potential to offer novel insights throughout the continuum of knee, foot, and ankle OA.

Spectral and photon-counting CT in OA imaging

Spectral CT is based on the principle that the attenuation of tissues depends not only on their density, but also on their atomic number Z, as well as on the energy of the photon beam.[66] Using these properties, spectral CT may be used in particular to characterize certain materials contained in tissues and to quantify them. Furthermore, spectral CT may provide monoenergetic images, in order to optimize image contrast and manage metal artifacts.[66]

Recent years have seen renewed interest in spectral CT, thanks to the implementation of dual-energy technology on clinical CT scanners. Dual-energy CT (DECT) is a subset of spectral CT, for which two X-ray energy spectra are used. Most commonly used applications of DECT in clinical routine, which are of interest in the field of OA include the workup of crystal-induced arthropathies, as well as the detection of bone marrow lesions on noncalcium CT.[67,68] Furthermore, DECT has been used to assess tendons, ligaments, and menisci but the diagnostic performance with current DECT technology is not on par with that obtained with MRI.[66]

Recently, a new type of CT system was introduced, based on photon-counting detectors that allow multi-energy imaging. Photon-counting (PC) detectors, opposite to energy-integrating (EI) detectors that have been used in CT systems so far, can count the number of incoming photons and measure their energy level.[69] Compared with EI-detectors, PC detectors are smaller in size, allowing for higher spatial resolution, and they have increased sensitivity, which allows for dose reduction, and in theory better material differentiation. Finally, they are less prone to beam-hardening artifacts.[69]

The increased spatial resolution is particularly interesting for the assessment of bone, including subchondral bone, which is thought to play an important part in the pathophysiology of OA.[70–72] Peña *et al.*[73] showed that bone mineral density and bone microstructural parameters could be measured with lower image noise and better reproducibility with photon-counting CT (PCCT) compared with energy-integrating CT (EICT). Similar performance in bone parameter measurements as EICT could further be achieved while decreasing the radiation dose by a factor of 2.3.

The higher resolution of PCCT should improve the detection and characterization of articular crystal deposits, and the improved performance of the detectors should in theory lead to improved differentiation between crystals compared with DECT, including the differentiation between hydroxyapatite and calcium pyrophosphate which is not achievable with current technology.[74]

In vitro studies have also shown the potential for compositional assessment of cartilage using PCCT. Different contrast agents may be used simultaneously to assess the composition of cartilage by targeting different molecular components.[75,76] There is ongoing research to overcome the remaining technical challenges associated with PCCT before widespread clinical implantation.

Advanced ultrasound imaging – shear wave elastography, contrast-enhanced ultrasound

There are several new sonographic techniques that can be applied to imaging of OA. Shear wave elastography (SWE) enables quantification of mechanical and elastic tissue properties. Shear waves propagate faster in stiffer and contracted tissues. Quantitative shear modulus maps are shown in a color-coded elastogram on an ultrasound screen. Shear wave velocities are measured in meters per second, and tissue elasticity is measured in kilopascals.[77] SWE has been applied to evaluate femoral cartilage in OA-affected knees,[78] abductor pollicis brevis and flexor pollicis brevis muscles in patients with thumb carpometacarpal OA,[79] vastus lateralis muscle in painful knee OA patients,[80] and in hamstring muscles of knee OA patients.[81] These studies showed differences of SWE values in the aforementioned anatomical structures between OA and non-OA patients,[78–81] as well as correlation with knee pain and physical function.[81]

Contrast-enhanced ultrasound provides the evaluation of dynamic blood perfusion *via* signals from a gas-filled microbubble contrast agent.[82] A prospective study included 31 patients with different degrees of radiographic knee OA.[83] All patients had grayscale ultrasound, power Doppler ultrasound, contrast-enhanced ultrasound for detection of synovitis in knee OA, using CE-MRI as reference. For synovitis scoring, grayscale ultrasound and contrast enhanced ultrasound were significantly correlated with CE-MRI ($p < 0.001$, and $p = 0.03$, respectively). Grayscale ultrasound had limited overall accuracy for detection of synovitis in knee OA; however, when it was combined with contrast power Doppler or contrast enhanced ultrasound, overall diagnostic performance improved for detection of mild synovitis, but not for moderate synovitis.

In summary, although there are several studies reporting the use of new sonographic imaging techniques in OA patients, those studies are predominantly preliminary in nature. Beyond demonstration of technical feasibility, more research is needed to validate its use in the clinical and research setting.

Application of artificial intelligence in imaging of OA

The use of artificial intelligence (AI), such as but not limited to deep learning and convoluted neural networks (CNN) has become popular in the OA research community. PubMed search conducted by the authors of this paper in August 2022 using the keywords 'osteoarthritis', 'deep learning', and 'artificial intelligence' yielded 109 papers, published between 2017 and 2022. Additional search using the keywords 'machine learning (173 papers)', 'transfer learning (181 papers)', 'convolutional neural network (66 papers)', 'Siamese neural network (5 papers)', and 'adversarial neural network (6 papers)' in combination with 'osteoarthritis' and 'imaging' was also performed. A recent systematic literature review published in March 2022 identified 46 publications (mostly published between 2017 and July 2021) that met inclusion criteria.[84] Papers describing the use of AI in knee OA comprised 85% of such papers, while hip OA filled the remaining 15%. Most of the studies used the data from the OAI or the Multicenter Osteoarthritis Study. Only 7% of the articles offered external validation. A variety of AI applications in the context of OA has been described in the literature, including the use of CNN for differentiating between advanced knee OA and subchondral insufficiency fractures,[85] automatic detection and classification of knee OA,[86] texture analysis of patella from X-rays for detection of patellofemoral OA,[87] large scale MRI-based morphological phenotyping of OA,[88] deep learning approach for prediction of pain progression in knee OA[89] as well as prediction of radiographic medial joint space loss over a 48-month period,[90] and automatic subregional assessment of knee cartilage degradation using quantitative T2 relaxometry and deep learning.[91] It has been postulated that the future vision of machine learning applications in OA imaging depends on the successful implementation of AI for improving the workflow of radiologists, with a higher level of precision and reproducibility.[92] Provision of risk assessment tools for individual patients may also play a key role in the era of precision medicine.[92] Potential pitfalls of AI-based methods include limited generalizability, AI model's reliability, and limited

interpretability of AI models.[93] It should be noted that developing field of AI can not only aid radiologists with the visual tasks of interpreting images, but also more practical view point such as improvement of workflows and noninterpretive tasks (such as optimization of protocoling, image reconstruction and enhancement) leading to improved efficiency of day-to-day work.[94]

Other novel techniques: multiscale X-ray phase contrast imaging, spectroscopic photoacoustic imaging of cartilage, and magnetic particle translation

There are other novel imaging techniques that do not fall into any of aforementioned categories. Multiscale X-ray phase contrast imaging (X-PCI) can discriminate regional extracellular matrix and cell alterations in soft tissues with homogeneous and uniform densities by exploiting both attenuated and refracted X-rays in the traversed tissue.[95,96] A previous study demonstrated that volumetric X-PCI-CT imaging of a fully preserved *ex vivo* human knee joint allows superior depiction and discrimination of soft tissues such as cartilage, ligaments, tendons, capsular structures, muscles and bone, compared with conventional CT and with similar differentiation of the structures compared to MRI.[97] A study by Horng *et al.*[95] demonstrated the potential of multiscale PCI-CT for evaluating chondral architecture and composition of 10 formalin-preserved healthy and moderately degenerated knee osteochondral samples, on a cellular and subcellular level with a 3D volumetric approach. X-PCI could resolve the three layers of the cartilage and the chondral architectural organization, with good correlation to histologic and transmission electron microscopy images. X-PCI can thus serve as a potential tool for investigating cartilage disease evolution in knee OA in a basic research setting. A major limitation of X-PCI is limited availability of the equipment (and lack of easy accessibility to a synchrotron facility), its lack of ability to image large objects and a trade-off between spatial resolution and radiation dose. Currently, submicron scale imaging is only feasible in an *ex vivo* or post-mortem laboratory setting.

Spectroscopic photoacoustic (sPA) imaging is an emerging hybrid technique, which takes advantages of optical (high optical contrast) and acoustic imaging (low acoustic attenuation in soft tissue).[98] sPA can image tissue composition based on the optical absorption contrast, and with adequate imaging depth and resolution of ultrasound, and easily distinguish between different tissue types.[98,99] Wu *et al.* explored the potential and possible clinical application of sPA imaging to characterize cartilage damage in OA. Using 15 pieces of chondral samples harvested at the time of total knee arthroplasty in OA patients, *ex vivo* sPA imaging was performed. The collagen-related PA spectral changes were clearly visible and were related to different severity of chondral damage, with good agreement with histology and the Mankin score.[98]

A technique to measure synovial fluid mechanics using magnetic nanoparticles has been proposed.[100] In an equine-based model of OA, magnetic particle translation in a given time within the synovial fluid sample collected from OA-affected joints was higher relative to synovial fluid collected from healthy joints. This study demonstrated technical feasibility of evaluating synovial fluid viscosity using limited volumes of synovial fluid sample collected from OA-affected joints.

In summary, technical feasibility of X-PCI and sPA has been demonstrated for evaluation of articular cartilage damage in OA. Magnetic particle translation may be used as a surrogate measure of synovial fluid mechanics. More work needs to be done before these techniques may be performed *in vivo*.

Conclusion

Several semiquantitative MRI analysis tools are available and can be applied to imaging of OA. In particular, ROAMES is specifically made to be used in MRI-based screening for structural definition of eligibility in clinical DMOAD trials. Technical developments in compositional imaging of articular cartilage continue to occur. Novel imaging techniques such as PET-MRI, advanced ultrasound, WB-CT, and spectral photon-counting CT are emerging in the OA research field. Advantages and disadvantages of each of these techniques are summarized in Table 2. Technical feasibility of X-PCI and sPA has been demonstrated for evaluation of cartilage in OA. In the current era of widespread AI research in OA imaging, it is hoped that the successful implementation of AI will improve the workflow of radiologists, as well as the level of precision and reproducibility in interpretation of images.

Table 2. Advantages and disadvantages of advanced imaging techniques of OA.

Advanced techniques	Advantages	Disadvantages
Compositional MRI	Detection of early (pre-morphologic) physiological change within cartilage to signify early OA Recent developments accelerating MR image acquisition and automating cartilage tissue segmentation have made it more feasible to use this technology to analyze larger imaging data sets	Limited availability of software to perform compositional MRI High cost Technical limitations associated with interpretation of values, intra- and inter-individual variabilities, the influence of vendors and the hardware, and software that makes comparability challenging, as well as the long MRI acquisition times and time-consuming analysis techniques The need for standardization of technique
PET-MRI	Offers unique abilities to provide quantitative information about molecular and metabolic activities, such as bone remodeling and inflammation, which are thought to be targets of disease-modifying OA therapies May be able to identify sources of musculoskeletal pain in OA	Radiation exposure High cost
Weight-bearing CT	Able to detect signs of OA incidence and progression missed by other imaging modalities Higher sensitivity to cartilage loss compared with standard CT More accurate than radiographs for assessing hind- and midfoot measurements	Radiation exposure Limited evaluation of soft tissue structures Limited availability of scanners
Spectral and photon-counting CT	*Spectral CT*: Characterization certain materials contained in tissues, and to quantify them Provision of monoenergetic images to optimize image contrast and manage metal artifacts Workup of crystal-induced arthropathies and detection of bone marrow lesions *Photon-counting CT*: Higher spatial resolution, increased sensitivity, lower radiation dose, & better material differentiation, compared with standard CT Less prone to beam-hardening artifacts	Radiation exposure Limited evaluation of soft tissue structures Limited availability of scanners
Advanced ultrasound imaging – shear wave elastography (SWE), contrast-enhanced ultrasound (CEUS)	SWE enables quantification of mechanical and elastic tissue properties CEUS provides the evaluation of dynamic blood perfusion Help differentiate between OA and non-OA patients	Operator dependency Unable to assess deep structures Limited ability to assess osseous structures Only preliminary literature evidence is available

CT, computed tomography; MR, magnetic resonance; MRI, magnetic resonance imaging; OA, osteoarthritis; PET-MRI, positron emission tomography–magnetic resonance imaging.

Declarations

ORCID iDs
Frank W. Roemer [iD] https://orcid.org/0000-0001-9238-7350

Thomas Link [iD] https://orcid.org/0000-0002-2850-8143

Ali Guermazi [iD] https://orcid.org/0000-0002-9374-8266

References

1. Hunter DJ, Guermazi A, Lo GH, *et al*. Evolution of semi-quantitative whole joint assessment of knee OA: MOAKS (MRI Osteoarthritis Knee Score). *Osteoarthritis Cartilage* 2011; 19: 990–1002.

2. Roemer FW, Frobell R, Lohmander LS, *et al*. Anterior Cruciate Ligament OsteoArthritis Score (ACLOAS): longitudinal MRI-based whole joint assessment of anterior cruciate ligament injury. *Osteoarthritis Cartilage* 2014; 22: 668–682.

3. Roemer FW, Collins J, Kwoh CK, *et al*. MRI-based screening for structural definition of eligibility in clinical DMOAD trials: rapid OsteoArthritis MRI Eligibility Score (ROAMES). *Osteoarthritis Cartilage* 2020; 28: 71–81.

4. Roemer FW, Demehri S, Omoumi P, *et al*. State of the art: imaging of osteoarthritis – revisited 2020. *Radiology* 2020; 296: 5–21.

5. Banuls-Mirete M, Lombardi AF, Posis AIB, *et al*. Effusion-synovitis worsening mediates the association between body mass index and Kellgren-Lawrence progression in obese individuals: data from the Osteoarthritis Initiative. *Osteoarthritis Cartilage* 2022; 30: 1278–1286.

6. Ramezanpour S, Kanthawang T, Lynch J, *et al*. Impact of sustained synovitis on knee joint structural degeneration: 4-year MRI data from the Osteoarthritis Initiative. *J Magn Reson Imaging*. Epub ahead of print 13 May 2022. DOI: 10.1002/jmri.28223

7. Mohajer B, Guermazi A, Conaghan PG, *et al*. Statin use and MRI subchondral bone marrow lesion worsening in generalized osteoarthritis: longitudinal analysis from Osteoarthritis Initiative data. *Eur Radiol* 2022; 32: 3944–3953.

8. Lee JJ, Namiri NK, Astuto B, *et al*. A personalized risk model leverages MRI-based structural phenotypes and clinical factors to predict incidence of radiographic osteoarthritis. *Arthritis Care Res (Hoboken)*. Epub ahead of print 4 March 2022. DOI: 10.1002/acr.24877

9. Roemer FW, Collins JE, Hunter DJ, *et al.* Patterns of progression differ between Kellgren-Lawrence 2 and 3 knees fulfilling different definitions of a cartilage-meniscus phenotype in the Foundation for National Institutes of Health Osteoarthritis Biomarkers Study (FNIH). *Osteoarthr Cartil Open* 2022; 4: 100284.

10. Sandford HJC, MacKay JW, Watkins LE, *et al.* Gadolinium-free assessment of synovitis using diffusion tensor imaging. *NMR Biomed* 2022; 35: e4614.

11. De Vries BA, Breda SJ, Sveinsson B, *et al.* Detection of knee synovitis using non-contrast-enhanced qDESS compared with contrast-enhanced MRI. *Arthritis Res Ther* 2021; 23: 55.

12. Yi J, Lee YH, Song HT, *et al.* Double-inversion recovery with synthetic magnetic resonance; a pilot study for assessing synovitis of the knee joint compared to contrast-enhanced magnetic resonance imaging. *Eur Radiol* 2019; 29: 2573–2580.

13. Zhong L, Li M, Du X, *et al.* Quantitative evaluation of the characteristic of infrapatellar fat pad Fat Content and Unsaturation Index by using hydrogen proton MR spectroscopy. *Magn Reson Imaging*. Epub ahead of print 31 July 2022. DOI: 10.1016/j.mri.2022.07.014.

14. Chen Y, Zhang X, Li M, *et al.* Quantitative MR evaluation of the infrapatellar fat pad for knee osteoarthritis: using proton density fat fraction and T2* relaxation based on DIXON. *Eur Radiol* 2022; 32: 4718–4727.

15. Li J, Fu S, Gong Z, *et al.* MRI-based texture analysis of infrapatellar fat pad to predict knee osteoarthritis incidence. *Radiology* 2022; 304: 611–621.

16. Link TM, Neumann J and Li X. Prestructural cartilage assessment using MRI. *J Magn Reson Imaging* 2017; 45: 949–965.

17. Roos EM and Arden NK. Strategies for the prevention of knee osteoarthritis. *Nat Rev Rheumatol* 2016; 12: 92–101.

18. Emanuel KS, Kellner LJ, Peters MJM, *et al.* The relation between the biochemical composition of knee articular cartilage and quantitative MRI: a systematic review and meta-analysis. *Osteoarthritis Cartilage* 2022; 30: 650–662.

19. Nieminen MT, Casula V and Nissi MJ. Compositional MRI of articular cartilage – current status and the way forward. *Osteoarthritis Cartilage* 2022; 30: 633–635.

20. Liebl H, Joseph G, Nevitt MC, *et al.* Early T2 changes predict onset of radiographic knee osteoarthritis: data from the osteoarthritis initiative. *Ann Rheum Dis* 2015; 74: 1353–1359.

21. Prasad AP, Nardo L, Schooler J, *et al.* T(1)rho and T(2) relaxation times predict progression of knee osteoarthritis. *Osteoarthritis Cartilage* 2013; 21: 69–76.

22. Razmjoo A, Caliva F, Lee J, *et al.* T2 analysis of the entire osteoarthritis initiative dataset. *J Orthop Res* 2021; 39: 74–85.

23. Owman H, Ericsson YB, Englund M, *et al.* Association between delayed gadolinium-enhanced MRI of cartilage (dGEMRIC) and joint space narrowing and osteophytes: a cohort study in patients with partial meniscectomy with 11 years of follow-up. *Osteoarthritis Cartilage* 2014; 22: 1537–1541.

24. Crema MD, Hunter DJ, Burstein D, *et al.* Association of changes in delayed gadolinium-enhanced MRI of cartilage (dGEMRIC) with changes in cartilage thickness in the medial tibiofemoral compartment of the knee: a 2 year follow-up study using 3.0 T MRI. *Ann Rheum Dis* 2014; 73: 1935–1941.

25. Brinkhof S, Nizak R, Khlebnikov V, *et al.* Detection of early cartilage damage: feasibility and potential of gagCEST imaging at 7T. *Eur Radiol* 2018; 28: 2874–2881.

26. Madelin G, Xia D, Brown R, *et al.* Longitudinal study of sodium MRI of articular cartilage in patients with knee osteoarthritis: initial experience with 16-month follow-up. *Eur Radiol* 2018; 28: 133–142.

27. Banjar M, Horiuchi S, Gedeon DN, *et al.* Review of quantitative knee articular cartilage MR imaging. *Magn Reson Med Sci* 2022; 21: 29–40.

28. Chaudhari AS, Kogan F, Pedoia V, *et al.* Rapid Knee MRI acquisition and analysis techniques for imaging osteoarthritis. *J Magn Reson Imaging* 2020; 52: 1321–1339.

29. Zhou Y, Pandit P, Pedoia V, *et al.* Accelerating T1rho cartilage imaging using compressed sensing with iterative locally adapted support detection and JSENSE. *Magn Reson Med* 2016; 75: 1617–1629.

30. Zibetti MVW, Sharafi A, Otazo R, *et al.* Accelerating 3D-T1rho mapping of cartilage using compressed sensing with different sparse and low rank models. *Magn Reson Med* 2018; 80: 1475–1491.

31. Kim J, Zhang CA, Yang M, *et al.* (eds). Highly accelerated T1ρ imaging using kernel-based low-rank compressed sensing reconstruction in knees with and without osteoarthritis. In: *Annual*

conference of International Society of Magnetic Resonance in Medicine (ISMRM), 2021, virtual.

32. Sharafi A, Zibetti MVW, Chang G, *et al.* 3D MR-Fingerprinting for rapid simultaneous T1, T2, and T1rho volumetric mapping of the human articular cartilage at 3T. *NMR Biomed* 2022; 35: e4800.

33. Li H, Yang M, Kim J, *et al.* SuperMAP: deep ultrafast MR relaxometry with joint spatiotemporal undersampling. *Magn Reson Med* 2023; 89: 64–76.

34. Desai AD, Caliva F, Iriondo C, *et al.* The International Workshop on Osteoarthritis Imaging Knee MRI Segmentation Challenge: a multi-institute evaluation and analysis framework on a standardized dataset. *Radiol Artif Intell* 2021; 3: e200078.

35. Ebrahimkhani S, Jaward MH, Cicuttini FM, *et al.* A review on segmentation of knee articular cartilage: from conventional methods towards deep learning. *Artif Intell Med* 2020; 106: 101851.

36. Gaj S, Yang M, Nakamura K, *et al.* Automated cartilage and meniscus segmentation of knee MRI with conditional generative adversarial networks. *Magn Reson Med* 2020; 84: 437–449.

37. Gatti AA and Maly MR. Automatic knee cartilage and bone segmentation using multi-stage convolutional neural networks: data from the osteoarthritis initiative. *MAGMA* 2021; 34: 859–875.

38. Liu F, Zhou Z, Jang H, *et al.* Deep convolutional neural network and 3D deformable approach for tissue segmentation in musculoskeletal magnetic resonance imaging. *Magn Reson Med* 2018; 79: 2379–2391.

39. Jena A, Taneja S, Rana P, *et al.* Emerging role of integrated PET-MRI in osteoarthritis. *Skeletal Radiol* 2021; 50: 2349–2363.

40. van den Wyngaert T, de Schepper S, Elvas F, *et al.* Positron emission tomography-magnetic resonance imaging as a research tool in musculoskeletal conditions. *Q J Nucl Med Mol Imaging* 2022; 66: 15–30.

41. Kogan F, Fan AP, McWalter EJ, *et al.* PET/MRI of metabolic activity in osteoarthritis: a feasibility study. *J Magn Reson Imaging* 2017; 45: 1736–1745.

42. Savic D, Pedoia V, Seo Y, *et al.* Imaging bone cartilage interactions in osteoarthritis using [18F]-NaF PET-MRI. *Mol Imaging* 2016; 15: 1–12.

43. Watkins L, MacKay J, Haddock B, *et al.* Assessment of quantitative [18F]Sodium fluoride PET measures of knee subchondral bone perfusion and mineralization in osteoarthritic and healthy subjects. *Osteoarthritis Cartilage* 2021; 29: 849–858.

44. Jena A, Goyal N, Rana P, *et al.* Differential 18F-NaF uptake in various compartments in knee osteoarthritis: an observational study using PET/MRI. *Clin Radiol* 2022; 77: 613–620.

45. Kobayashi N, Inaba Y, Tateishi U, *et al.* Comparison of 18F-fluoride positron emission tomography and magnetic resonance imaging in evaluating early-stage osteoarthritis of the hip. *Nucl Med Commun* 2015; 36: 84–89.

46. Lohmander LS, Englund PM, Dahl LL, *et al.* The long-term consequence of anterior cruciate ligament and meniscus injuries: osteoarthritis. *Am J Sports Med* 2007; 35: 1756–1769.

47. Kogan F, Fan AP, Monu U, *et al.* Quantitative imaging of bone-cartilage interactions in ACL-injured patients with PET-MRI. *Osteoarthritis Cartilage* 2018; 26: 790–796.

48. Tibrewala R, Bahroos E, Mehrabian H, *et al.* [18F]-sodium fluoride PET/MR imaging for bone-cartilage interactions in hip osteoarthritis: a feasibility study. *J Orthop Res* 2019; 37: 2671–2680.

49. Tibrewala R, Pedoia V, Bucknor M, *et al.* Principal component analysis of simultaneous PET-MRI reveals patterns of bone-cartilage interactions in osteoarthritis. *J Magn Reson Imaging* 2020; 52: 1462–1474.

50. MacKay JW, Watkins L, Gold G, *et al.* [18F]NaF PET-MRI provides direct in-vivo evidence of the association between bone metabolic activity and adjacent synovitis in knee osteoarthritis: a cross-sectional study. *Osteoarthritis Cartilage* 2021; 29: 1155–1162.

51. Haddock B, Fan AP, Uhlrich SD, *et al.* Assessment of acute bone loading in humans using [18F]NaF PET/MRI. *Eur J Nucl Med Mol Imaging* 2019; 46: 2452–2463.

52. Watkins LE, Haddock B, Mackay J, *et al.* Evaluating changes in bone mineralization and perfusion in response to acute exercise in an osteoarthritic population. In: *2020 International workshop on osteoarthritis imaging*, Salzburg, 2020, Abstract book, p. 71. https://www.isoai.org/_files/ugd/ee317a_77ce377668774716a336ff6117325820.pdf

53. Hirata Y, Inaba Y, Kobayashi N, *et al.* Correlation between mechanical stress by finite element analysis and 18F-fluoride PET uptake in hip osteoarthritis patients. *J Orthop Res* 2015; 33: 78–83.

54. Watkins L, Mackay J and Kogan F. Areas of altered [18F]NaF PET Uptake in response to

exercise show OA progression on MRI over 2 years. In: *2021 international workshop on osteoarthritis imaging*, Rotterdam, 2021, Abstract book, p. 22. https://www.isoai.org/_files/ugd/ac154b_10095b12170a46eea3680c885b9b6d00.pdf

55. Nguyen BJ, Burt A, Baldassarre RL, *et al*. The prognostic and diagnostic value of 18F-FDG PET/CT for assessment of symptomatic osteoarthritis. *Nucl Med Commun* 2018; 39: 699–706.

56. Stumpe KD, Romero J, Ziegler O, *et al*. The value of FDG-PET in patients with painful total knee arthroplasty. *Eur J Nucl Med Mol Imaging* 2006; 33: 1218–1225.

57. Cipriano PW, Lee SW, Yoon D, *et al*. Successful treatment of chronic knee pain following localization by a sigma-1 receptor radioligand and PET/MRI: a case report. *J Pain Res* 2018; 11: 2353–2357.

58. Segal NA, Nevitt MC, Lynch JA, *et al*. Diagnostic performance of 3D standing CT imaging for detection of knee osteoarthritis features. *Phys Sportsmed* 2015; 43: 213–220.

59. Kvarda P, Heisler L, Krahenbuhl N, *et al*. 3D assessment in posttraumatic ankle osteoarthritis. *Foot Ankle Int* 2021; 42: 200–214.

60. Fritz B, Fritz J, Fucentese SF, *et al*. Three-dimensional analysis for quantification of knee joint space width with weight-bearing CT: comparison with non-weight-bearing CT and weight-bearing radiography. *Osteoarthritis Cartilage* 2022; 30: 671–680.

61. Guermazi A, Niu J, Hayashi D, *et al*. Prevalence of abnormalities in knees detected by MRI in adults without knee osteoarthritis: population based observational study (Framingham Osteoarthritis Study). *BMJ* 2012; 345: e5339.

62. Segal NA, Frick E, Duryea J, *et al*. Correlations of medial joint space width on fixed-flexed standing computed tomography and radiographs with cartilage and meniscal morphology on magnetic resonance imaging. *Arthritis Care Res (Hoboken)* 2016; 68: 1410–1416.

63. Segal NA, Murphy MT, Everist BM, *et al*. Clinical value of weight-bearing CT and radiographs for detecting patellofemoral cartilage visualized by MRI in the MOST study. *Osteoarthritis Cartilage* 2021; 29: 1540–1548.

64. Segal NA, Rabe KG, Lynch JA, *et al*. Detection of meniscal extrusion: comparison of standing computed tomography to non-loaded magnetic resonance imaging. *Osteoarthritis Cartilage* 2018; 26: S441–S442.

65. Burssens ABM, Buedts K, Barg A, *et al*. Is lower-limb alignment associated with hindfoot deformity in the coronal plane? A weightbearing CT analysis. *Clin Orthop Relat Res* 2020; 478: 154–168.

66. Omoumi P, Becce F, Racine D, *et al*. Dual-Energy CT: basic principles, technical approaches, and applications in musculoskeletal imaging (Part 1). *Semin Musculoskelet Radiol* 2015; 19: 431–437.

67. Omoumi P, Zufferey P, Malghem J, *et al*. Imaging in gout and other crystal-related arthropathies. *Rheum Dis Clin North Am* 2016; 42: 621–644.

68. Omoumi P, Verdun FR, Guggenberger R, *et al*. Dual-Energy CT: basic principles, technical approaches, and applications in musculoskeletal imaging (Part 2). *Semin Musculoskelet Radiol* 2015; 19: 438–445.

69. Willemink MJ, Persson M, Pourmorteza A, *et al*. Photon-counting CT: technical principles and clinical prospects. *Radiology* 2018; 289: 293–312.

70. Burr DB and Gallant MA. Bone remodelling in osteoarthritis. *Nat Rev Rheumatol* 2012; 8: 665–673.

71. Omoumi P, Babel H, Jolles BM, *et al*. Relationships between cartilage thickness and subchondral bone mineral density in non-osteoarthritic and severely osteoarthritic knees: in vivo concomitant 3D analysis using CT arthrography. *Osteoarthritis Cartilage* 2019; 27: 621–629.

72. Omoumi P, Babel H, Jolles BM, *et al*. Quantitative regional and sub-regional analysis of femoral and tibial subchondral bone mineral density (sBMD) using computed tomography (CT): comparison of non-osteoarthritic (OA) and severe OA knees. *Osteoarthritis Cartilage* 2017; 25: 1850–1857.

73. Peña JA, Klein L, Maier J, *et al*. Dose-efficient assessment of trabecular microstructure using ultra-high-resolution photon-counting CT. *Z Med Phys*. Epub ahead of print 18 May 2022. DOI: 10.1016/j.zemedi.2022.04.001.

74. Bernabei I, Sayous Y, Raja AY, *et al*. Multi-energy photon-counting computed tomography versus other clinical imaging techniques for the identification of articular calcium crystal deposition. *Rheumatology (Oxford)* 2021; 60: 2483–2485.

75. Paakkari P, Inkinen SI, Honkanen MKM, *et al*. Quantitative dual contrast photon-counting computed tomography for assessment of articular cartilage health. *Sci Rep* 2021; 11: 5556.

76. Baer K, Kieser S, Schon B, *et al*. Spectral CT imaging of human osteoarthritic cartilage via quantitative assessment of glycosaminoglycan content using multiple contrast agents. *APL Bioeng* 2021; 5: 026101.

77. Taljanovic MS, Gimber LH, Becker GW, *et al*. Shear-wave elastography: basic physics and musculoskeletal applications. *Radiographics* 2017; 37: 855–870.

78. Yokuş A, Toprak M, Arslan H, *et al*. Evaluation of distal femoral cartilage by B-mode ultrasonography and shear wave elastography in patients with knee osteoarthritis: a preliminary study. *Acta Radiol* 2021; 62: 510–514.

79. Nwawka OK, Weinstock-Zlotnick G, Lin B, *et al*. Association of clinical assessments of hand function and quantitative ultrasound metrics in first carpometacarpal osteoarthritis. *HSS J* 2020; 16(Suppl. 2): 420–424.

80. Yagi M, Taniguchi M, Tateuchi H, *et al*. Relationship between individual forces of each quadriceps head during low-load knee extension and cartilage thickness and knee pain in women with knee osteoarthritis. *Clin Biomech (Bristol, Avon)* 2022; 91: 105546.

81. Li F, Wang ZY, Zhang ZJ, *et al*. In hamstring muscles of patients with knee osteoarthritis an increased ultrasound shear modulus indicates a permanently elevated muscle tonus. *Front Physiol* 2022; 12: 752455.

82. Ntoulia A, Barnewolt CE, Doria AS, *et al*. Contrast-enhanced ultrasound for musculoskeletal indications in children. *Pediatr Radiol* 2021; 51: 2303–2323.

83. de Vries BA, Breda SJ, Meuffels DE, *et al*. Diagnostic accuracy of grayscale, power Doppler and contrast-enhanced ultrasound compared with contrast-enhanced MRI in the visualization of synovitis in knee osteoarthritis. *Eur J Radiol* 2020; 133: 109392.

84. Binvignat M, Pedoia V, Butte AJ, *et al*. Use of machine learning in osteoarthritis research: a systematic literature review. *RMD Open* 2022; 8: e001998.

85. Klontzas ME, Vassalou EE, Kakkos GA, *et al*. Differentiation between subchondral insufficiency fractures and advanced osteoarthritis of the knee using transfer learning and an ensemble of convolutional neural networks. *Injury* 2022; 53: 2035–2040.

86. Abdullah SS and Rajasekaran MP. Automatic detection and classification of knee osteoarthritis using deep learning approach. *Radiol Med* 2022; 127: 398–406.

87. Bayramoglu N, Nieminen MT and Saarakkala S. Machine learning based texture analysis of patella from X-rays for detecting patellofemoral osteoarthritis. *Int J Med Inform* 2022; 157: 104627.

88. Namiri NK, Lee J, Astuto B, *et al*. Deep learning for large scale MRI-based morphological phenotyping of osteoarthritis. *Sci Rep* 2021; 11: 10915.

89. Guan B, Liu F, Mizaian AH, *et al*. Deep learning approach to predict pain progression in knee osteoarthritis. *Skeletal Radiol* 2022; 51: 363–373.

90. Guan B, Liu F, Haj-Mirzaian A, *et al*. Deep learning risk assessment models for predicting progression of radiographic medial joint space loss over a 48-month follow-up period. *Osteoarthritis Cartilage* 2020; 28: 428–437.

91. Thomas KA, Krzemiński D, Kidziński Ł, *et al*. Open source software for automatic subregional assessment of knee cartilage degradation using quantitative t2 relaxometry and deep learning. *Cartilage* 2021; 13(1_suppl): 747S–756S.

92. Joseph GB, McCulloch CE, Sohn JH, *et al*. AI MSK clincal applications: cartilage and osteoarthritis. *Skeletal Radiol* 2022; 51: 331–343.

93. Caliva F, Namiri NK, Dubreuil M, *et al*. Studying osteoarthritis with artificial intelligence applied to magnetic resonance imaging. *Nat Rev Rheumatol* 2022; 18: 112–121.

94. Shin Y, Kim S and Lee YH. AI musculoskeletal clinical applications: how can AI increase my day-to-day efficiency. *Skeletal Radiol* 2022; 51: 293–304.

95. Horng A, Stroebel J, Geith T, *et al*. Multiscale X-ray phase contrast imaging of human cartilage for investigating osteoarthritis formation. *J Biomed Sci* 2021; 28: 42.

96. Bravin A, Coan P and Suortti P. X-ray phase-contrast imaging: from pre-clinical applications towards clinics. *Phys Med Biol* 2013; 58: R1–R35.

97. Horng A, Brun E, Mittone A, *et al*. Cartilage and soft tissue imaging using X-rays: propagation-based phase-contrast computed tomography of the human knee in comparison with clinical imaging techniques and histology. *Invest Radiol* 2014; 49: 627–634.

98. Wu M, van Teeffelen BCJ, Ito K, *et al*. Spectroscopic photoacoustic imaging of cartilage damage. *Osteoarthritis Cartilage* 2021; 29: 1071–1080.

99. Lei H, Johnson LA, Liu S, *et al*. Characterizing intestinal inflammation and fibrosis in Crohn's disease by photoacoustic imaging: feasibility study. *Biomed Opt Express* 2016; 7: 2837.

100. Shah YY, Maldonado-Camargo L, Patel NS, *et al*. Magnetic particle translation as a surrogate measure for synovial fluid mechanics. *J Biomech* 2017; 60: 9–14.